




Short Communication

# Nanoporous zirconia microspheres prepared by salt-assisted spray drying



M. Skovgaard<sup>1</sup> · M. Gudik-Sørensen<sup>2</sup> · K. Almdal<sup>3</sup> · A. Ahniyaz<sup>4</sup> 

Received: 11 November 2019 / Accepted: 20 March 2020 / Published online: 1 April 2020

© The Author(s) 2020 

## Abstract

Nanoporous zirconia with high surface area and crystallinity has a wide range of industrial applications, such as in inorganic exchangers for ion exchange columns, catalyst substrates, and packing material for HPLC. Spherical particles of crystalline nanoporous zirconia are highly desired in various industries due to easy handling of the materials in a fluidized bed. Here, spray drying was adopted to produce spherical nanoporous zirconia powders in both laboratory scale and pilot plant scale. Effect of salts on spray-dried  $ZrO_2$  powders and their crystallization behavior was studied. It was found that addition of salts to the zirconia precursors has a huge effect on the crystallization of nanoporous zirconia powders. These results have a great impact on the development of microspheres of nanocrystalline  $ZrO_2$  and potentially open up a new opportunity to the low-cost production of porous ceramic microspheres with the salt templating method, in general.

**Keywords** Nanoporous materials ·  $ZrO_2$  · Salt-assisted spray drying · Nanomaterials · Ceramics · Dental materials

## 1 Introduction

In the last couple of decades, zirconia has gained increasing interest, due to its mechanical properties, ability to catalyze chemical reactions and ionic conductivity at high temperature. For this reason, zirconia and zirconia doped with various metal oxides, such as yttria, ceria, and magnesia, have been widely studied [1]. Zirconia exhibits three crystallographic phases with increasing temperature at atmospheric pressure: monoclinic below 1175 °C, tetragonal between 1175 and 2370 °C and cubic above 2370 °C. Furthermore, a metastable tetragonal phase exists at room temperature. However, the metastable tetragonal zirconia phase transforms to the stable monoclinic phase due to a range of external factors: applied shear stresses [2], aging in humid atmosphere [3] or annealing [4]. The tetragonal-to-monoclinic phase transformation is associated with a volume expansion of ~ 4 vol%. This volume expansion is

the cause of the excellent mechanical properties of doped zirconia ceramics, as the stress-induced phase transformation of metastable tetragonal zirconia grains at the crack tips is the basis of transformation toughening in zirconia ceramics [5].

Porous zirconia with high surface area is of interest for various functional applications. Spherical micron sized-porous zirconia is of particular interest due to the reduced particle aggregation and free-flowing properties. Both alcohol drying [6] and spray drying [7] are known from the literature, and spray drying is furthermore widely used in various industries due to the easy operation and high reproducibility of the process. Another way to obtain small zirconia particles is by modifying of the precursor blend. Salt-assisted spray drying was tested as a possible route. It is known from the literature that salt-assisted spray drying and salt-assisted spray pyrolysis can be used to produce nano-sized ceramic particles [8].

✉ A. Ahniyaz, anwar.ahniyaz@ri.se; K. Almdal, kral@dtu.dk | <sup>1</sup>AAK Sweden AB, Västra Kajen, 37482 Karlshamn, Sweden. <sup>2</sup>Department of Energy Conversion and Storage, Technical University of Denmark, Frederiksborgvej 399, 4000 Roskilde, Denmark. <sup>3</sup>Department of Chemistry, Technical University of Denmark, Kemitorvet, 2800 Kgs. Lyngby, Denmark. <sup>4</sup>Division of Bioscience and Materials, RISE Research Institutes of Sweden, Stockholm, Sweden.



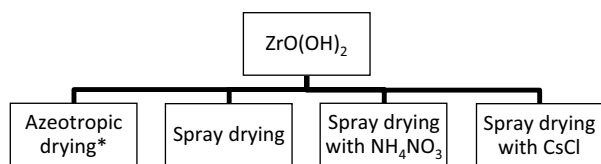


**Fig. 1** The tested azeotropic and aqueous spray drying preparation routes (\*dried with isopropanol)

In this study, first, different ways to prepare nano-sized zirconia particles were investigated. The tested preparation routes are azeotropic drying, spray drying of pure  $\text{ZrO}(\text{OH})_2$  and spray drying in combination with either  $\text{CsCl}$  or  $\text{NH}_4\text{NO}_3$ . An overview of the tested methods is illustrated in Fig. 1. The effect on particle size, crystal size, surface area, crystallization temperature, and crystal phase of the formed zirconia is studied.

## 2 Experimental

All chemicals were supplied by Aldrich, and they were all used as received. Dispersions of highly porous  $\text{ZrO}(\text{OH})_2$  powders were synthesized as previously described [9, 10] by controlled hydrolysis of  $\text{ZrOCl}_2$  and conditioning. The  $\text{ZrO}(\text{OH})_2$  powders are extremely porous and have specific surface area of  $\sim 350 \text{ m}^2/\text{g}$ .

### 2.1 Spray drying of neutral, aqueous dispersions

The pilot-scale spray dryer was used to spray drying of pure zirconia and  $\text{CsCl}$  salt containing zirconia, while the laboratory-scale spray drier was used to produce  $\text{NH}_4\text{NO}_3$  salt containing zirconia.

A suspension of amorphous  $\text{ZrO}(\text{OH})_2$  was prepared as described above. From the suspension, three different aqueous dispersions of  $\text{ZrO}(\text{OH})_2$  were prepared by stirring, with low ( $\text{ICsZrO}_2$ ) and high ( $\text{hCsZrO}_2$ )  $\text{CsCl}$  concentration and one without addition of  $\text{CsCl}$ . The pure  $\text{ZrO}_2$  precursor was spray dried without further preparation. The  $\text{ICsZrO}_2$  precursor solution was prepared by stirring 4 L 5.0 wt%  $\text{ZrO}(\text{OH})_2$  water suspension with 100 g  $\text{CsCl}$  until the salt was dissolved. The  $\text{hCsZrO}_2$  precursor solution was prepared by stirring 4 L 5.0 wt%  $\text{ZrO}(\text{OH})_2$  aqueous suspension with 200 g  $\text{CsCl}$  until the salt was dissolved. The dispersions were spray dried at pilot plant scale. Dispersions of amorphous zirconia in water were spray dried in a MOBILE MINOR™ Pilot Plant with an overall chamber diameter of 0.8 m, a cylindrical height of 0.83 m and a  $60^\circ$  cone. Droplets of the precursor solution were generated in the spraying chamber using a two-flow spray-nozzle with a replaceable orifice with a diameter of 1.5 mm. At drying temperatures 275/145 °C (inlet/outlet), dry-looking

powders were obtained. The produced powder was calcined at various temperatures.

Originally, it was expected to be possible to wash the salts out with anhydrous methanol. However, the solubility of the salt was too low, and the salt was instead removed with water to facilitate characterization of the particles.

### 2.2 Spray drying of acidic, aqueous dispersions

Dispersions containing high ( $\text{hNZrO}_2$ ) and low ( $\text{INZrO}_2$ ) concentrations of  $\text{NH}_4\text{NO}_3$  were prepared. The  $\text{hNZrO}_2$  precursor solution was prepared by mixing 200 g 5.0 wt%  $\text{ZrO}(\text{OH})_2$  water suspension, 200 ml ethanol (99.7%), 10 g acetic acid, 100 g ammonium nitrate, and 8 g of 2.0 M  $\text{HCl}$ . The resultant suspension was sonicated for 30 min with Vibracell before spray drying.

The  $\text{INZrO}_2$  precursor solution was prepared by mixing 200 g 5.0 wt%  $\text{ZrO}(\text{OH})_2$  water suspension, 200 ml ethanol (99.7%), 10 g acetic acid, 5 g ammonium nitrate, and 5 g of 2.0 M  $\text{HCl}$ . The resultant suspension was sonicated for 30 min with Vibracell before spray drying. The precursor solutions were spray dried at laboratory scale in a laboratory-scale spray drying reactor, which consists of a spraying chamber combined with a tube furnace and a filter [11]. Droplets of the precursor solution were generated in the spraying chamber using a two-flow spray-nozzle with a replaceable orifice with a diameter of 1.5 mm at room temperature of 25 °C. The liquid flow and gas flow were set to 1.76 ml/min and 16,000 ml/min, respectively. Outlet oven temperature was 280 °C, and dry-looking white spherical powders were collected. The produced powder was calcined at various temperatures. A schematic illustration of the custom-made laboratory-scale spray drier is shown in Fig. 2. At the end of the spray drying process,

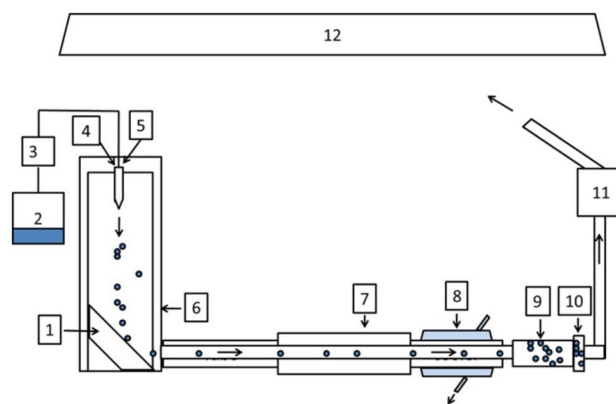


**Fig. 2** Schematic illustration of spray drying setup developed at the Research Institutes of Sweden (RISE). 1. PVC panel; 2. reactants; 3. pump; 4.  $\text{N}_2$  gas; 5. nozzle; 6. protective tube; 7. furnace; 8. water cooler; 9. particle collector; 10. filter bag; 11. exhaust pump; 12. fumehood

powder samples were collected with collector. With this laboratory-scale spray drier, 50–100 g powder samples can be easily collected on a daily basis. The scaled-up version of the similar set up is available at Cabot Corporation (USA) for a larger pilot-scale production of powders.

### 2.3 Calcination and washing

The samples were calcined in dry air at temperatures varying from 450 to 550 °C. After calcination, the crystalline samples were cooled to RT in ambient atmosphere. The CsCl and NH<sub>4</sub>NO<sub>3</sub> containing samples were washed with water until no reaction with AgNO<sub>3</sub> or nitrate sticks was observed. The washed samples were dried at RT in ambient atmosphere.

## 2.4 Characterization

### 2.4.1 XRD

A STOE theta–theta X-ray diffractometer, STOE and Cie GmbH, Darmstadt, Germany, was used in reflection mode, and XRD patterns were scanned in 0.1 steps ( $2\theta$ ) in the  $2\theta$  range from 20° to 60°, with a fixed counting time (30 s). The XRD patterns were analyzed using WinX<sup>POW</sup> software. For the crystalline samples, the obtained values of the t-ZrO<sub>2</sub> and m-ZrO<sub>2</sub> volume fractions ( $v_t$  and  $v_m$ ) were compared with the values obtained from the integral intensities of the monoclinic diffraction lines (–1 1 1) and (1 1 1) and the tetragonal diffraction line (1 0 1), following a procedure proposed by Toraya et al. [12]. The crystal size was calculated using the Scherrer equation [13].

### 2.4.2 Transmission electron microscopy (TEM)

Low- and high-resolution TEM images and selected area electron diffraction (SAED) patterns were obtained using a JEOL JEM-3010 microscope operating at 300 kV (Cs = 0.6 mm, Point resolution 0.17 nm). Images were recorded with a CCD camera (MultiScan model 794, Gatan, 1024 × 1024 μm) at a magnification of 4000–400,000 times. TEM samples were prepared by applying a drop of zirconia–isopropanol dispersion onto a carbon-coated Cu grid, and the solvent was allowed to slowly evaporate at room temperature.

### 2.4.3 Differential scanning calorimetry (DSC)

Differential scanning calorimetry was carried out using a high-sensitivity differential scanning calorimeter Seiko SII-DSC120 and a Seiko SII-DSC320. The samples (15–25 mg) were placed in aluminum pans with a mass of about 16 mg. Heating rate of 5 °C min<sup>–1</sup>. During all the

experiments, a protection gas of pure He (99.996%) was used with flow rate of 100 cm<sup>3</sup>/min. The DSC equipment is regularly temperature calibrated to within 0.5 °C using Zn metal.

### 2.4.4 Scanning electron microscopy (SEM)

In this study, an XL30 TMP environmental scanning electron microscope (ESEM) from Philips/FEI was used. In sample preparation, small amounts of powders were placed on an aluminum sample holder using a spatula. The ESEM investigation was carried out at room temperature (ca 25 °C) without sample coating. Accelerating voltage of 20–30 kV was used. The probe current (spot size) was varied between 4 and 6 nA, and the working distance (WD) was around 10 mm.

## 3 Results and discussion

The effects of preparation methods and the presence of either salts or isopropanol during calcination are listed in Table 1. It is observed that the different methods result in zirconia powders with very different properties. This means that the preparation route has a large effect on the properties of the produced zirconia powders; particularly, the crystal phase and crystal size are influenced. For the CsCl-containing samples, the crystallization temperature is also effected.

The XRD patterns for the samples calcined at 450 °C are illustrated in Fig. 3. It is observed that the (101) tetragonal reflection at  $2\theta = 30.2^\circ$  is more dominating for hNZrO<sub>2</sub> compared with INZrO<sub>2</sub> and the two pure samples, which have more dominating (–111) and (111) monoclinic reflections. The difference in peak width is a result of different crystal sizes. This difference is most pronounced when

**Table 1** Crystal size in nanometers, calcination temperature, monoclinic volume fraction ( $v_m$ ) of the spray-dried and azeotropic samples and crystallization temperature (from DSC)

Sample	Crystal size (nm)	Calcination temp. (°C)	$v_m$	Crystallization temp. (°C)
Azeotropic-dried	5.5	450	0.68	433
Spray-dried ZrO <sub>2</sub> (pilot scale)	7.2	450	0.69	435
hCsZrO <sub>2</sub> (pilot scale)	7.1	550	0.23	525
ICsZrO <sub>2</sub> (pilot scale)	7.5	550	0.27	525
hNZrO <sub>2</sub> (laboratory scale)	11.6	450	0.10	437
INZrO <sub>2</sub> (laboratory scale)	13.7	450	0.65	437

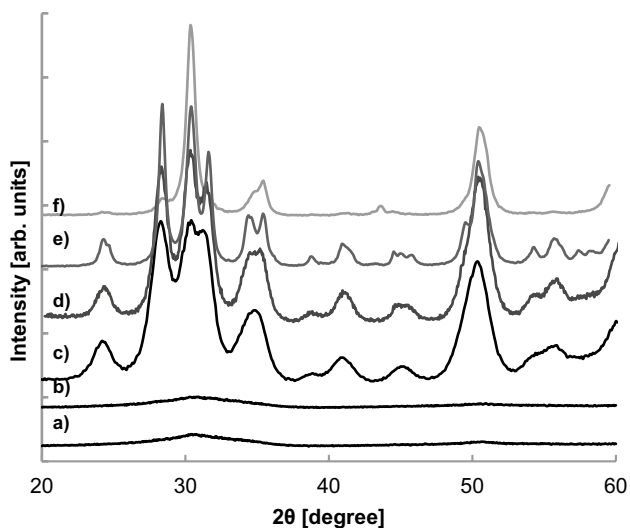


**Fig. 3** XRD patterns of powders calcined at 450 °C; (a)  $\text{ICsZrO}_2$ , (b)  $\text{hCsZrO}_2$ , (c) alcohol-dried zirconia, (d) spray dried pure zirconia, (e)  $\text{INZrO}_2$  and (f)  $\text{hNZrO}_2$

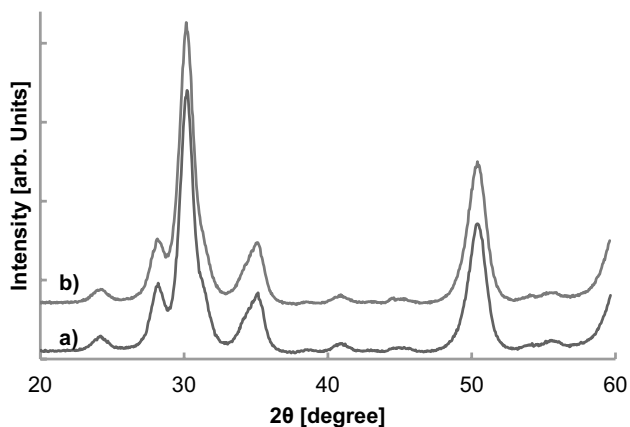
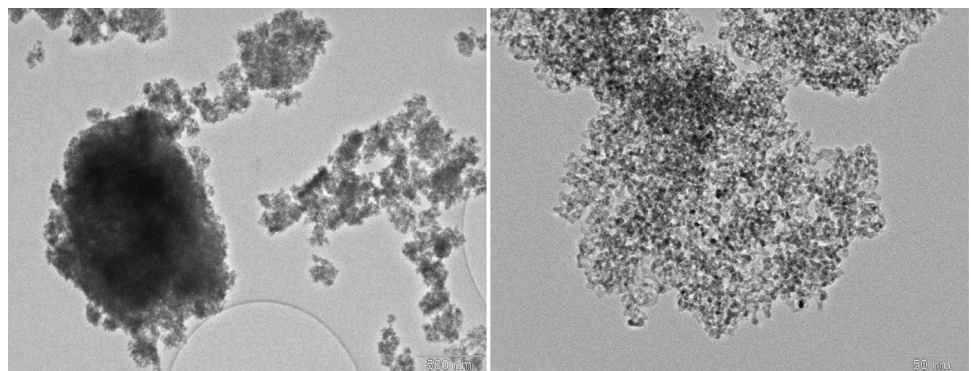


**Fig. 4** XRD patterns of zirconia spray-dried with CsCl calcined at 550 °C; (a)  $\text{ICsZrO}_2$  and (b)  $\text{hCsZrO}_2$

**Fig. 5** TEM pictures of calcined zirconia powder (from azeotropic dried samples)



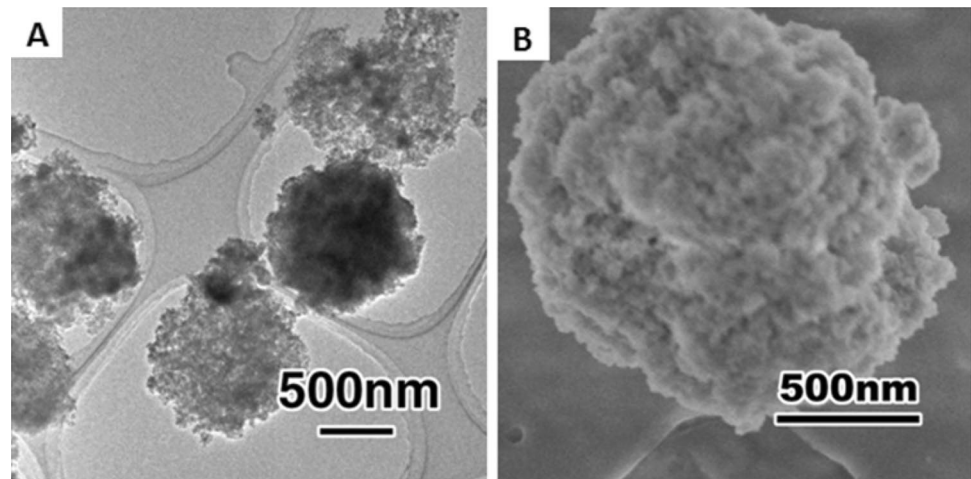
comparing the XRD patterns of the alcohol-dried sample and  $\text{INZrO}_2$  (Fig. 3c, e). The alcohol-dried sample has the broadest peaks because it has the smallest crystal size. Furthermore, it is found that while both the pure zirconia samples and the two samples spray dried with  $\text{NH}_4\text{NO}_3$  are crystalline at 450 °C, this is not the case for the two CsCl containing samples, which still are amorphous at this temperature. For this reason, these two samples were calcined at 550 °C and subjected to XRD. The results are illustrated in Fig. 4. It is observed that the tetragonal reflection is dominating for both samples.

The XRD patterns of the powders prepared with salt-assisted spray drying show only the existence of zirconia peaks and none of the peaks corresponding to CsCl or  $\text{NH}_4\text{NO}_3$  are observed. This result indicates that all the salt is removed during washing.

All the samples were analyzed with SEM and TEM. The azeotropic drying resulted in particles with a diffuse morphology (Fig. 5), whereas spray drying resulted for all samples in spherical particles with a diameter in the range of 1–2  $\mu\text{m}$  for the pure sample and for the samples spray dried with CsCl (Figs. 6, 7a–d). For the two samples spray-dried with  $\text{NH}_4\text{NO}_3$ , the particle sizes were in the range of < 0.5  $\mu\text{m}$  (Fig. 7e–h). The two  $\text{NH}_4\text{NO}_3$ -containing samples gave the widest particle size distributions. Except for the size differences, no changes in morphology were observed with either SEM or TEM in any of the spray dried samples.

All the tested methods resulted in crystalline nanoporous zirconia powders with particle sizes up to 2  $\mu\text{m}$ . This is in contrast to the very large and hard agglomerates of zirconia obtained by just calcining the air-dried  $\text{ZrO}(\text{OH})_2$  dispersion (not shown).

The two pure zirconia samples have similar properties, but azeotropic drying gives the smallest crystals and micron-sized particles with a more diffuse structure. Spray drying, however, gives micron sized spherical zirconia. Both methods give pure zirconia with primarily the monoclinic phase and the samples contain only 30 vol% tetragonal crystals. From the DSC analysis, the crystallization

**Fig. 6** TEM and SEM images of spray-dried pure ZrO<sub>2</sub>

temperature is found for the samples and it is observed that both the pure zirconia samples crystallize at  $\sim 435$  °C.

Salt-assisted spray drying with CsCl lowers the monoclinic volume fraction in the zirconia samples. Both CsCl-containing samples have lower  $v_m$  than the pure zirconia sample (see Table 1). The crystallization temperatures are, however, increased, and the two CsCl-containing samples crystallize at 525 °C. Calcination at 550 °C was expected to increase the sintering of the zirconia samples and hence increase the crystal size, but the crystal size does not increase significantly in any of the two samples and does not differ significantly from the spray-dried pure zirconia sample. The decrease in  $v_m$  is probably a result of anionic stabilization originating from incorporation of Cl<sup>-</sup> in the tetragon crystal lattice. The stabilizing effect is among others described by Gutzov et al. [14]. Furthermore, chloride ions adsorb strongly on zirconia and are difficult to remove completely from the surface [15].

In contrast to the CsCl containing samples, the presence of NH<sub>4</sub>NO<sub>3</sub> during calcination causes no increase in the crystallization temperature, as both the samples crystallize at  $\sim 435$  °C. For the two NH<sub>4</sub>NO<sub>3</sub>-containing samples, a significant difference is observed. hNZrO<sub>2</sub> has a volume fraction of monoclinic crystals ( $v_m$ ) of 0.10, whereas INZrO<sub>2</sub> has a  $v_m$  of 0.65. The latter is close to the  $v_m$  of the two pure zirconia samples (Table 1). In addition, the crystal sizes vary in these two samples and hNZrO<sub>2</sub> has a crystal size of 11.6 nm and INZrO<sub>2</sub> a size of 13.7 nm. These crystal sizes were confirmed by TEM. Both samples show increased crystal sizes compared with all the other samples. In particular, the sample containing the lowest content of NH<sub>4</sub>NO<sub>3</sub> has increased crystal size.

hNZrO<sub>2</sub> gives the lowest  $v_m$ , but has larger crystals, than the pure zirconia samples. This indicates a stabilization of the tetragonal phase, which most likely originates from ammonium ions working as mineralizers, in the same way, as chlorine ions stabilize the samples calcined in the

presence of CsCl. The stabilizing effect of ammonium ions counteracts the size effect and increases the critical size of the tetragonal crystals. Normally when the crystal size increases, the  $v_m$  will increase as well. This is not the case in this study and supports the presence of ammonium stabilization. Surprisingly, INZrO<sub>2</sub> is not stabilized to the same extent and is the one of all the salt-containing samples with the highest  $v_m$ . INZrO<sub>2</sub> and ICsZrO<sub>2</sub> have the same zirconia concentration, and the fact that only the CsCl is able to stabilize the tetragonal phase in the crystals strengthens hypothesis that the chloride ions have a stabilizing effect on the tetragonal phase.

In contrast to the diffuse particle structure of the samples dried with azeotropic distillation, all the spray-dried samples are spherical, but with different sizes depending on the production process. This indicates that the morphology and size are more a result of processing parameters, than a result of the properties and concentrations of the salts. Furthermore, the fact that the two NH<sub>4</sub>NO<sub>3</sub>-containing samples gave a wider particle size distribution supports this conclusion.

## 4 Conclusion

Salt-assisted spray drying method has been developed for the pilot-scale production of nanoporous zirconia microspheres.

Four different preparation routes were tested to prepare spherical zirconia powders: azeotropic drying with isopropanol, spray drying and salt-assisted spray drying with NH<sub>4</sub>NO<sub>3</sub> or CsCl (two different concentrations in both cases). From the results of this study, it is concluded that addition of high amounts of NH<sub>4</sub>NO<sub>3</sub> gives the crystals with the lowest monoclinic volume fraction and particles having a spherical shape. Spray drying of a precursor solution containing 1:1 ZrO<sub>2</sub>:CsCl results in almost the

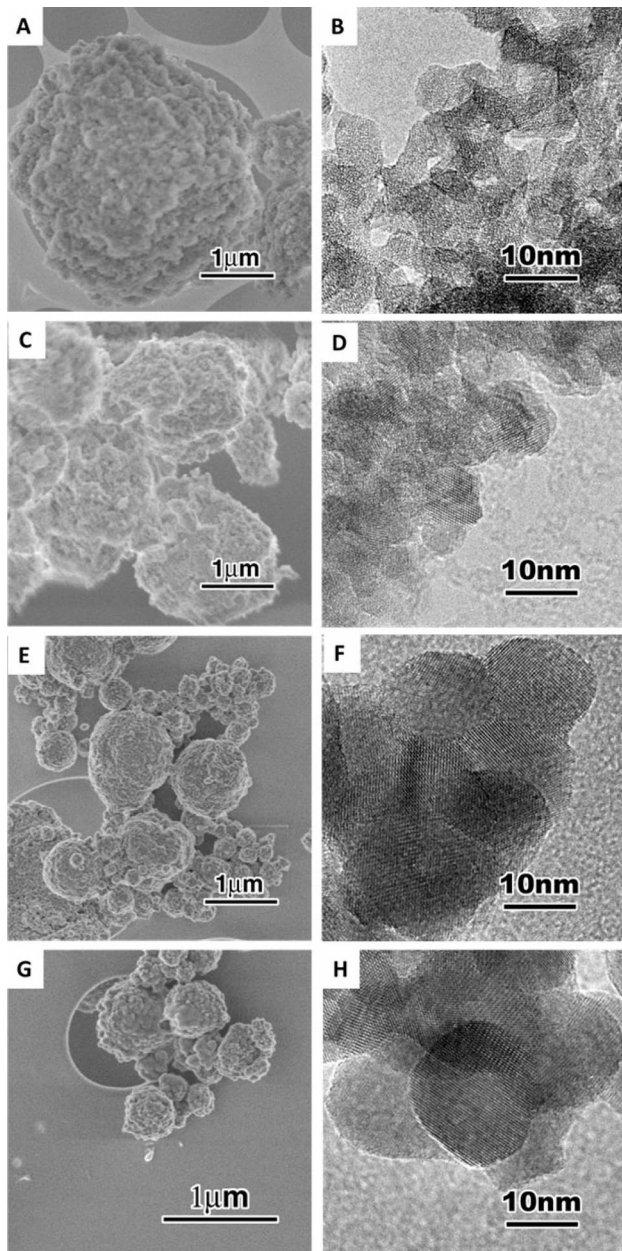


**Fig. 7** SEM and TEM of salt-assisted spray dried  $ZrO_2$ , **a, b**  $hCsZrO_2$ , **c, d**  $ICsZrO_2$ , **e, f**  $hNZrO_2$  and **g, h**  $INZrO_2$

same properties, but gives a little higher monoclinic volume fraction and a little smaller crystal size. These results have a great impact on the development of microspheres of nanocrystalline  $ZrO_2$  and potentially open up a new opportunity to the low-cost production of other porous ceramic microspheres with a salt templating method in general.

**Acknowledgements** Open access funding provided by RISE Research Institutes of Sweden. Financial support from DentoFit A/S and RISE Research Institutes of Sweden is gratefully acknowledged.

## Compliance with ethical standards

**Conflict of interest** The authors declare that they have no conflict of interest.

**Open Access** This article is licensed under a Creative Commons Attribution 4.0 International License, which permits use, sharing, adaptation, distribution and reproduction in any medium or format, as long as you give appropriate credit to the original author(s) and the source, provide a link to the Creative Commons licence, and indicate if changes were made. The images or other third party material in this article are included in the article's Creative Commons licence, unless indicated otherwise in a credit line to the material. If material is not included in the article's Creative Commons licence and your intended use is not permitted by statutory regulation or exceeds the permitted use, you will need to obtain permission directly from the copyright holder. To view a copy of this licence, visit <http://creativecommons.org/licenses/by/4.0/>.

## References

- Kelly PM, Rose LRF (2002) The martensitic transformation in ceramics—its role in transformation toughening. *Prog Mater Sci* 47:463–557
- Skovgaard M, Ahniyaz A, Sørensen BF, Almdal K, van Lelieveld A (2010) Effect of microscale shear stresses on the martensitic phase transformation of nanocrystalline tetragonal zirconia powders. *J Eur Ceram Soc* 30:2749–2755
- Skovgaard M, Almdal K, van Lelieveld A (2010) Phase stabilizing effects of phosphates and sulfates on nanocrystalline metastable tetragonal zirconia. *J Mater Sci* 45(22):6271–6274
- Garvie RC (1965) Occurrence of metastable tetragonal zirconia as a crystallite size effect. *J Phys Chem* 69:1238–1243
- Hannink RHJ, Kelly PM, Muddle BC (2000) Transformation toughening in zirconia-containing ceramics. *J Am Ceram Soc* 83:461–487
- Lin JD, Duh JG, Chiou BS (2001) The influence of washing and calcination condition on urea-derived ceria-yttria-doped tetragonal zirconia powders. *Mater Chem Phys* 68:42–55
- Shi JL, Gao JH, Lin ZX, Yan DS (1993) Effect of agglomerates in  $ZrO_2$  powder compacts on microstructural development. *J Mater Sci* 28:342–348
- Xia B, Lenggono IW, Okuyama K (2001) Novel route to nanoparticle synthesis by salt-assisted aerosol decomposition. *Adv Mater* 13:1579–1582
- Van Lelieveld A, Almdal K, Linderroth S, Sorensen BF (2005) Composite material useful as dental filling material and in medicine for dentistry comprises filler and polymerizable resin base. WO2005099652-A1; NO200604920-A; EP1737415-A1; AU2005232365-A1; CN1950053-A; BR200509889-A; MX2006011038-A1; JP2007532589-W; KR2007015946-A; EP1737415-B1; US2008119585-A1; DE602005006549-E; EP1952793-A2; ZA200608230-A; KR858373-B1; ES2307170-T3
- Nielsen MS, Van Lelieveld A (2010) Dental filling material, useful in dentistry, comprises filler comprising metastable zirconia particles with surface functionalities, in a tetragonal and/or cubic crystalline phase, and a polymerizable resin base. WO2010049522-A2
- Andersson N, Alberius PCA, Pedersen JS, Bergstrom L (2004) Structural features and adsorption behaviour of mesoporous silica particles formed from droplets generated in a spraying chamber. *Microporous Mesoporous Mater* 72:175–183

12. Toraya H, Yoshimura M, Somiya S (1984) Calibration curve for quantitative-analysis of the monoclinic-tetragonal  $ZrO_2$  system by X-ray-diffraction. *J Am Ceram Soc* 67:C119–C121
13. Scherrer P (1918) Determination of the size and internal structure of colloidal particles using X-rays. *Nachr Ges Wiss Göttingen* 2:98–100
14. Gutzov S, Ponahlo J, Lengauer CL, Beran A (1994) Phase characterization of precipitated zirconia. *J Am Ceram Soc* 77:1649–1652
15. Amphlett CB, McDonald LA, Redman MJ (1958) Synthetic inorganic ion-exchange materials. 2. Hydrous zirconium oxide and other oxides. *J Inorg Nucl Chem* 6:236–245

**Publisher's Note** Springer Nature remains neutral with regard to jurisdictional claims in published maps and institutional affiliations.